Geology Publications   Faculty and Staff Scholarship

2010

Climate in the Southern Sawatch Range and Elk Mountains, Colorado, U.S.A., during the Last Glacial Maximum: Inferences Using a Simple Degree-Day Model

Keith A. Brugger
University of Minnesota, Morris

Follow this and additional works at: https://digitalcommons.morris.umn.edu/geol_facpubs

Part of the Geology Commons, and the Glaciology Commons

Recommended Citation

Climate in the Southern Sawatch Range and Elk Mountains, Colorado, U.S.A., during the Last Glacial Maximum: Inferences Using a Simple Degree-Day Model

Keith A. Brugger*

**Geology Discipline, University of Minnesota Morris, Morris, Minnesota 56267, U.S.A.
bruggeka@morris.umn.edu*

Abstract

Equilibrium-line altitudes (ELAs) were determined from reconstructions of 22 paleoglaciers at their extent during the local last glacial maximum (LGM) using the accumulation-area method. LGM ELAs thus derived ranged from 2980 to 3560 m and follow a statistically significant regional trend of rising $\sim$4.5 m km^{-1} to the east. Two approaches using a degree-day model were used to infer LGM climate by finding plausible combinations of temperature and precipitation change that (1) would be required to lower ELAs to their mean LGM values in both the Taylor Park/eastern Elk Mountains region and western Elk Mountains, and (2) provide steady-state mass balances to maintain individual glaciers. The results of these two approaches are convergent and suggest that in the absence of significant changes in precipitation, mean summer (or mean annual) temperatures within the study area during the LGM were on the order of about 7 °C cooler than at present. The model also suggests that even allowing for modest changes in LGM precipitation ($\pm$25%), the required mean summer temperature depressions are within $\sim$0.5 °C of these values. Furthermore, there appears to be no significant dependence on small potential changes in temperature seasonality (i.e., winter temperatures). The inferred magnitude of LGM temperature change in the study area is consistent with other estimates from the broader Southern and Central Rocky Mountain region.

Introduction

Records of paleoclimate have increasingly led to a better understanding of climate dynamics and the response of ecosystems and other Earth systems to climate variability. In addition, paleoclimate data have provided both "benchmarks" against which models used for projecting future climate change can be tested, and insights as to the kinds of environments those changes may bring (Oldfield and Alverson, 2003). Nevertheless, additional research is needed to quantify the magnitude and the spatial and temporal patterns of past climate change. This is particularly true for the last glacial maximum (LGM) in the Rocky Mountains (Pierce, 2004), where questions concerning its timing and regional differences in the magnitude of temperature and/or precipitation change remain (Hostetler and Clark, 1997; Licciardi et al., 2004; Thackray et al., 2004; Munroe et al., 2006).

In this paper, a simple degree-day model is used to estimate climatic conditions that existed during the local LGM in the southern Sawatch Range and Elk Mountains in central Colorado (Fig. 1). The model was originally used (Brugger, 2006) to infer paleoclimate based on equilibrium-line altitudes (ELAs) of five lobes of the Taylor River Glacier Complex (the Taylor River and Spring Creek Lobes, and the Rocky Brook, Trail Creek, and Bushwhack Glaciers shown in Fig. 2); however, the present analysis expands its application to a wider geographic area in order to examine regional climate change. The model is also used to explore sensitivity of the ELAs of paleoglaciers to changes in temperature, precipitation, and seasonality of temperature changes during the LGM. Degree-day or other temperature-indexed methods for simulating snow and ice melt perform well over basin-sized spatial scales and time intervals exceeding a couple of days (Hock, 1999, 2003). A recent analysis by Ohmura (2001) suggests

that the success of these methods is due largely to long-wave atmospheric radiation and sensible heat flux being the most important sources of heat energy, both of which are strongly influenced by the air temperature above the glacier. Thus, degree-day approaches have the advantages of requiring far less parameterization than more physically based energy-balance models, being computationally simple, and can be better justified for situations when complete meteorological (or climate) data are lacking (Braithwaite and Zhang, 2000; Hock, 2003). Consequently, degree-day modeling has been widely used to simulate glacier mass balance (e.g., Woo and Fitzharris, 1992; Braithwaite, 1995; Jóhannesson et al., 1995; Hock, 1999; Casal et al., 2004) as means of mass-balance forcing for modeling the response of glaciers and ice sheets to climate change (e.g., Huybrechts and Oerlemans, 1990; Jóhannesson, 1997; Oerlemans et al., 1998; Braithwaite and Zhang, 1999, 2000; Marshall et al., 2002; Flowers et al., 2005) and for estimating the contribution of glacier melt to sea-level changes (e.g., Raper et al., 2000; Huybrechts, 2002; Braithwaite and Raper, 2002; Wild et al., 2003; DeWoul and Hock, 2005; Raper and Braithwaite, 2006). To a lesser extent, degree-day methods have also been used specifically to infer paleoclimate (Hostetler and Clark, 2000; Kull and Grosjean, 2000; Vincent et al., 2005; Brugger, 2006; Hughes and Braithwaite, 2008).

Methods

RECONSTRUCTION OF GLACIERS IN THE STUDY AREA AND ESTIMATES OF ELAS

ELAs were determined from reconstructions of the LGM extent of 22 glaciers that existed in the study area (Fig. 2). The
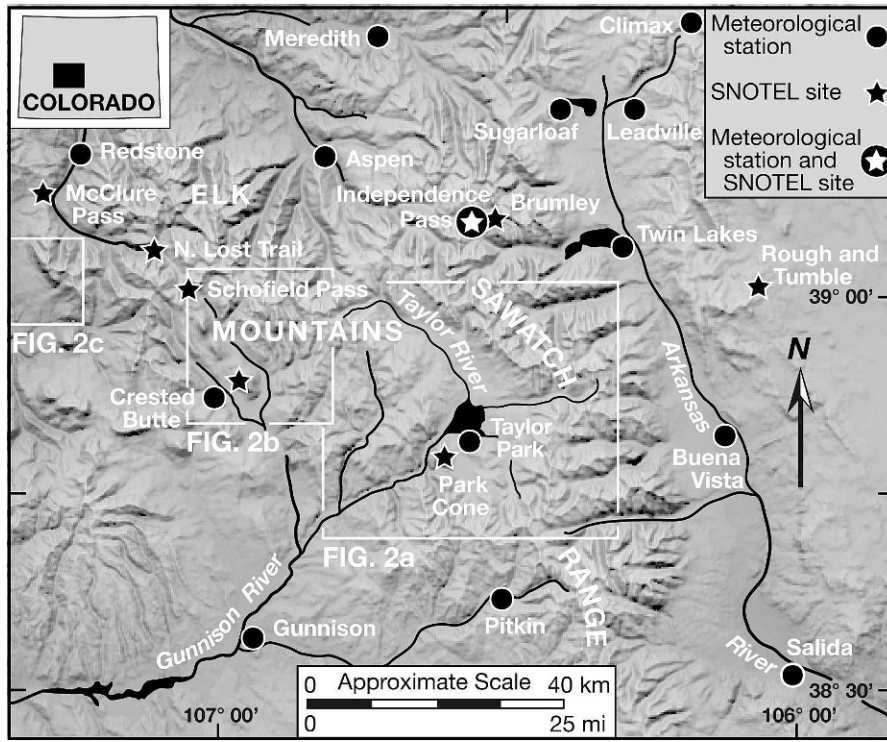
FIGURE 1. Shaded-relief map of the study area in central Colorado showing the location of meteorological stations and SNO-TEL sites from which modern climate data was obtained.

LGM is locally dated between 16.1 and 20.8 ka based on zero-erosion, [10]Be ages obtained from boulders on a terminal moraine complex in the Taylor Valley (Brugger, 2007). Ice extent in individual valleys was determined by detailed field mapping of moraine geometry, the distribution of erratic boulders, indicators of the direction of ice flow (e.g., roches moutonnées, streamlined bedrock), and the upper limit of glacial erosion. Mapping was supplemented by analyses of topographic and geologic maps, aerial photos, and/or digital elevation models. Ice-surface contours were constructed with due consideration of the elevation of the ice margin, local ice flow direction, and general convergent and divergent flow in, respectively, the accumulation and ablation areas. Minor adjustments were made iteratively to ensure ice thickness and surface slopes along flow lines yielded basal shear stresses that fell within 50–150 kPa (Paterson, 1994). ELAs for the reconstructed glaciers were found using the accumulation-area ratio (AAR) method using a ratio of 0.65 ± 0.05 (Porter, 1975; Meierding, 1982; Torsnes et al., 1993).

THE DEGREE-DAY MODEL

The model was briefly described previously (Brugger, 2006), but several additional details are presented here. The specific net mass-balance $b_n(z)$ at an elevation z is

$$b_n(z) = \int_{t_1}^{t_2} P_s(t,z) + M(t,z)dt \qquad (1)$$

where $M(t,z)$ is the rate of ice or snow melt and $P_s(t,z)$ is the rate of snow precipitation at the glacier's surface during the interval t_1 to t_2 that represents the hydrologic year (1 October to 30 September). Although the refreezing of melt- and/or rainwater as a source of internal accumulation has been treated explicitly and with varying degrees of sophistication in some degree-day or energy-balance models (e.g., Laumann and Reeh, 1993; Jóhannesson et al., 1995; Marshall et al., 2002), it is ignored here as it has been elsewhere

(e.g., Klein et al., 1999; Braithwaite and Zhang, 2000). Refreezing water typically contributes little (≤10%) to a glacier's mass balance (Trabant and Mayo, 1985; Östling and Hooke, 1986; Miller and Pelto, 1999); however, this process does in some cases account for a very significant fraction of mass gain. Its omission in the model used here is addressed in subsequent sensitivity analyses. Refreezing of rainwater during warmer months can also enhance melting through the release of latent heat, but it is not incorporated in the model. In general this contributes little to total melting (Ohno and Nakawo, 1998). Finally, any internal or basal melting (due to strain heating, viscous dissipation of energy flowing in conduits, and so forth) is also ignored. Thus surface melt is assumed to be equivalent to net ablation and snow precipitation equivalent to net accumulation. By definition $b_n(z_{ELA}) = 0$ where z_{ELA} is the equilibrium-line altitude.

Equation (1) is in fact numerically integrated and thus becomes

$$b_n(z) = \sum_{m=1}^{12} \left[P_{s_m}(z) - \sum_{d=1}^{n} M_d(z) \right] \qquad (2)$$

where $P_{s_m}(z)$ is the monthly snow precipitation and $M_d(z)$ is the daily melt at z, and n is the number of days in month m. (The daily summation of temperatures and monthly summation of precipitation values reflects the temporal resolution of available climate data.) Melt is related to mean daily air temperature $T_d(z)$ through a degree-day factor d_f

$$M_d(z) = \begin{cases} d_f T_d(z) & T_d(z) > 0°C \\ 0 & T_d(z) \leq 0°C \end{cases} \qquad (3)$$

Values of d_f for ice and snow are taken here as 0.0080 ± 0.001 and 0.0045 ± 0.001 m w.e. (water equivalent) d^{-1} °C^{-1}, respectively, which are close to the mean values determined for relatively debris-free snow and ice on modern glaciers (Table 1). Initially d_f for snow is used, but at any time in the modeled hydrologic year when snow melt exceeds snow accumulation, it is
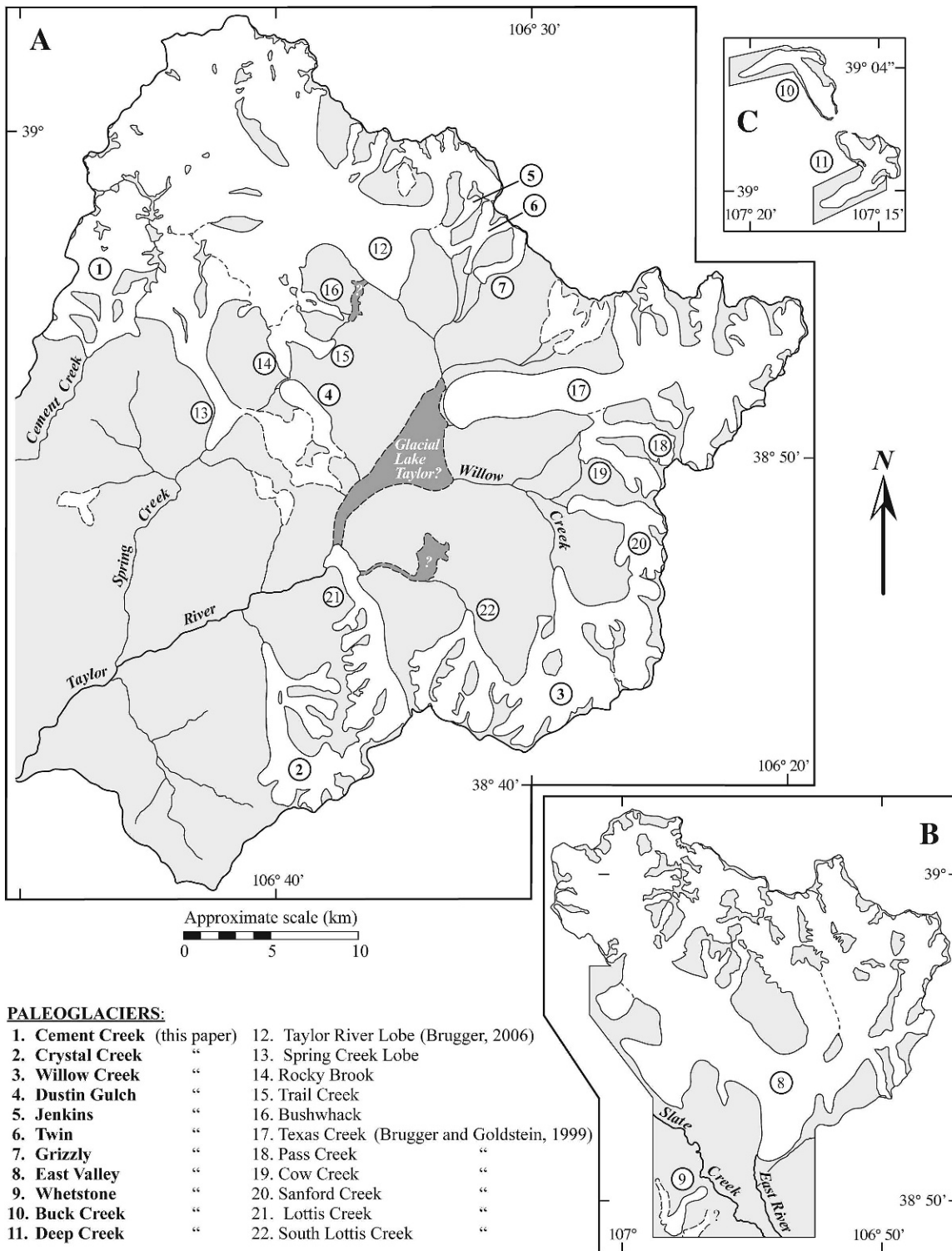
FIGURE 2. Paleoglaciers of the (a) Taylor River basin and adjacent Cement Creek, (b) East River drainage and Whetstone Mountain, and (c) Deep and Buck Creeks during the LGM. Dashed lines defining glacier boundaries indicate uncertainty due to incomplete fieldwork or unresolved problems. Dashed lines within larger glaciers show the position of major ice divides. Glacial lakes are speculative.

PALEOGLACIERS:

1. **Cement Creek** (this paper)	12. Taylor River Lobe (Brugger, 2006)	
2. **Crystal Creek** "	13. Spring Creek Lobe	
3. **Willow Creek** "	14. Rocky Brook	
4. **Dustin Gulch** "	15. Trail Creek	
5. **Jenkins** "	16. Bushwhack	
6. **Twin** "	17. Texas Creek (Brugger and Goldstein, 1999)	
7. **Grizzly** "	18. Pass Creek "	
8. **East Valley** "	19. Cow Creek "	
9. **Whetstone** "	20. Sanford Creek "	
10. **Buck Creek** "	21. Lottis Creek "	
11. **Deep Creek** "	22. South Lottis Creek "	

replaced with that for ice. No allowance is made for potential changes in d_f over a melt season (cf. Hock, 2003), nor is it assumed *a priori* that snow and ice surfaces are exceptionally debris laden.

Monthly snow precipitation is

$$P_s(z) = fP_{mod}(z)Fp \qquad (4)$$

where $P_{mod}(z)$ is the modern mean monthly precipitation at z, and F_p is the prescribed fractional change in precipitation. Modern

monthly precipitation is calculated by

$$P_{mod}(z) = (z - z_{REF})\frac{dP}{dz} + P(z_{REF}) \qquad (5)$$

where z_{REF} is some reference elevation where precipitation P is known, and dP/dz is the vertical precipitation gradient. The empirically derived, temperature-dependent partitioning function f used in Equation (4) to determine that fraction of the monthly

TABLE 1
Measured or derived degree-day factors (d_f) for snow and ice in glacial environments.

Location	d_f (mm w.e. d^{-1} °C^{-1}) Ice	Snow	Reference
Weissfluhjoch, Switzerland		4.5	(Zingg, 1951)[2]
Greenland Ice Sheet	8.5[1]		(Schytt, 1955)[3]
Various Swiss glaciers	6.0[1]		(Kasser, 1959)[2]
Greenland Ice Sheet	18.6		(Ambach, 1963)[2]
Spitsbergen	13.8		(Schytt, 1964)[2]
Ålfotbreen, Norway	7.5		(NVE, 1965)[4]
Andrews Glacier, United States		4.3	Outcalt and MacPhail, 1965
Storsteinsfjellbreen, Norway	7.5		Pytte and Liestøl, 1966
Storbreen, Norway	5.5		(Liestøl, 1967)[2]
Supphellebreen, Norway	6.3		(Orheim, 1970)[2]
Fillefjell, Norway		3.9	(Furmyr and Tollan, 1975)[4]
Various Norwegian glaciers	5.5[1]		(Braithwaite, 1977)[2]
Weissfluhjoch, Switzerland		4.5	(De Quervain, 1979)[2]
White, Sverdrup Glaciers, Arctic Canada	6.3[1]		(Braithwaite, 1981)[2]
Aletschgletscher, Switzerland	11.7	5.3	(Lang, 1986)[3]
Qamanârssûp sermia, West Greenland	7.7[1]		Braithwaite and Olesen, 1989
Greenland Ice Sheet (margin)	12.6[1]		(Van der Wal, 1992)[3]
Franz Josef Glacier, New Zealand	6.0	3.0	Woo and Fitzharris, 1992
Qamanârssûp sermia, West Greenland	7.9[1]		Braithwaite and Olesen, 1993
Ålfotbreen, Norway	6.0	4.5	Laumann and Reeh, 1993
Nigardsbreen, Norway	5.5	4.0	Laumann and Reeh, 1993
Hellstugubreen, Norway	5.5	3.5	Laumann and Reeh, 1993
Qamanârssûp sermia, West Greenland	8.3	3.7	Braithwaite, 1995
Nordbogletscher, West Greenland	8.1	2.9	Braithwaite, 1995
Sátujökull, Iceland	7.7	5.6	Jóhannesson et al., 1995
Nigardsbreen, Norway	6.4	4.4	Jóhannesson et al., 1995
Qamanârssûp sermia, West Greenland	7.3	2.8	Jóhannesson et al., 1995
Moreno Glacier, Patagonia	7.0[1]		(Takeuchi et al., 1996)[2]
Australian Alps		2.9	Whetton et al., 1996
Dokrriani Glacier, Himalaya		5.9	(Singh and Kumar, 1996)[3]
Blöndujökull, Kvíslajökull, Iceland	5.0	4.5	Jóhannesson, 1997
Illvirajökull, Iceland	7.6	5.6	Jóhannesson, 1997
Glacier de Sarennes, France	6.2	3.8	(Vincent and Vallon, 1997)[2]
Glacier Upsala, Patagonia	7.1		Naruse et al., 1997
Kronprins Christian Land, North Greenland	9.8		(Braithwaite et al., 1998)[2]
Han Tausen Land, North Greenland	5.9		(Braithwaite et al., 1998)[2]
John Evans Glacier, Canada	7.1[1]	4.0[1]	(Arendt and Sharp, 1999)[3]
Storglaciären, Sweden	6.3	4.4	Hock, 1999
South Cascade Glacier, United States	6.2[1]		Tangborn, 1999
Greisgletscher, Switzerland	8.9[1]		Braithwaite and Zhang, 2000
Glacier AX010, Himalaya	9.2[1]	8.5[1]	(Kayastha et al., 2000a)[3]
Khumbu Glacier, Himalaya	16.9		(Kayastha et al., 2000b)[3]
Rakiot Glacier, Himalaya	6.6		(Kayastha et al., 2000b)[3]
Dokrriani Glacier, Himalaya	7.4	5.7	(Singh et al., 2000)[3]
Rabots Glaciär, Sweden	6.8	4.7	Refsnider and Brugger, 2001
Yala Glacier, Himalaya	9.7[1]		(Kayastha, 2001)[3]
Saint Sorlin Glacier, France		4.0	Vincent, 2002
Yala Glacier, Himalaya	9.3[1]		Kayastha, et al., 2003
Dongkemadi Glacier, Tibetan Plateau	13.8[1]		Kayastha, et al., 2003
July 1st Glacier, Tibetan Plateau	7.2[1]		Kayastha, et al., 2003
Means	8.1 ± 3.0	4.4 ± 1.2	

[1] Mean of several or a range of values, sometimes measured at different times and elevations.
[2] Cited in Braithwaite and Zhang (2000).
[3] Cited in Hock (2003).
[4] Cited in Laumann and Reeh (1993).
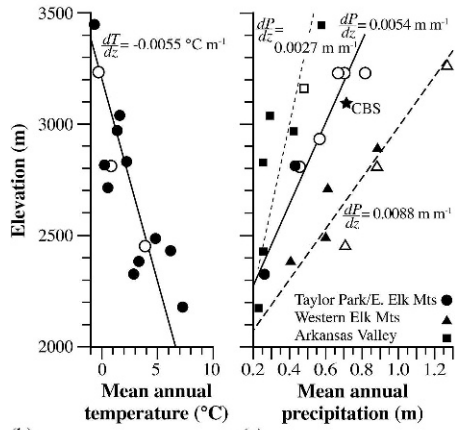
precipitation that falls as snow has the form

$$f = \left(1 + e^{c(T_m(z) - T_{crit})}\right)^{-1} \qquad (6)$$

where $T_m(z)$ is now the monthly mean air temperature. The

constants c and T_{crit} were determined for each area using monthly snow depth data (Fig. 3a) and available snow density data. The latter indicate that the densities of monthly snowfall are quite consistent, averaging ~67.0 ± 6 kg m^{-3}. Equation (6) yields a continuous function that ensures there is a mean monthly
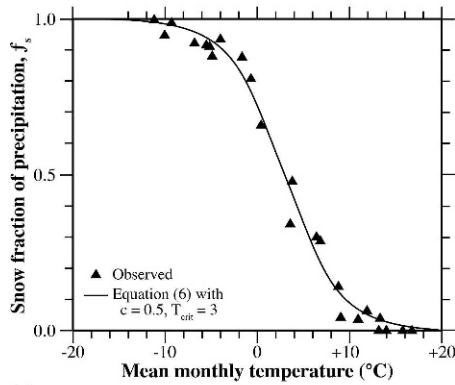
FIGURE 3. (a) Fraction of monthly precipitation that falls as snow as a function of mean monthly temperature in the western Elk Mountains. Data from the Taylor Park/eastern Elk Mountains has a similar form. See text for discussion. Altitudinal dependence of (b) temperature and (c) precipitation that define the temperature lapse rate and vertical precipitation gradient(s). In (c) precipitation data have been segregated by region. See text for discussion and statistical significance of regressions. Filled and open symbols in both (b) and (c) are NCDC and non-NCDC norms, respectively.

temperature below which all precipitation for that month falls as snow, and another above which as rain. For temperatures between these values, snowfall will be some fraction of total monthly precipitation. Other modeling studies have treated precipitation as being either all rain or all snow according to some critical air temperature (e.g., Laumann and Reeh, 1993; Jóhannesson et al., 1995; Casal et al., 2004; Flowers et al., 2005) by using a linear relationship to represent the transition between these extremes (e.g., Klein et al., 1999) or by using a probability function approach (e.g., Braithwaite and Zhang, 2000; Marshall et al, 2002). Finally, analyses designed to test the sensitivity of the model results to assumed changes in precipitation (discussed subsequently) imply that the exact values assigned to the constants in the partitioning function are not too critical.

Mean daily air temperatures are assumed to vary sinusoidally about the mean annual temperature $T_a(z)$

$$T_d(z) = A_y \sin\left(\frac{2\pi d}{\lambda} - \phi\right) + T_a(z) \qquad (7)$$

where A_y is the amplitude of yearly temperature variations, d is the day of year, λ is the period (365 d), and ϕ is the phase angle (taken here as ~1.93 rad so yearly maximum and minimum temperatures

in the model match those observed). A_y and $T_a(z)$ are given by

$$A_y = (T_{Jul}(z_{REF}) + \Delta T_{Jul}) - (T_{Jan}(z_{REF}) + \Delta T_{Jan}) \qquad (8)$$

$$T_a(z) = (z - z_{REF})\frac{dT}{dz} + T_a(z_{REF}) \qquad (9)$$

where $T_{Jul}(z_{REF})$, $T_{Jan}(z_{REF})$, and $T_a(z_{REF})$ are, respectively, the modern mean July, January, and annual air temperatures at z_{REF}, ΔT_{Jul} and ΔT_{Jan} are the prescribed temperature perturbations, and dT/dz is the lapse rate for mean annual temperature.

IMPLEMENTATION OF THE MODEL

The model is used in two ways to infer climate during the LGM in the study area: first by introducing perturbations in temperature (ΔT_{Jul} and ΔT_{Jan}) and precipitation (F_p) and then using Equation (2) to find the equilibrium-line altitude, where $b_n(z_{ELA}) = 0$, by iteration; and second by varying the perturbations so that the net mass balance B_n of a reconstructed paleoglacier is

$$B_n = \int_A b_n dA \approx \sum_{i=1}^{j} b_{n_i} A_i = 0 \qquad (10)$$

where A is the glacier's area, composed of j number of discrete intervals, and b_{n_i} is the mean specific net-balance over A_i.

Modern meteorological data from 14 stations (available at the Western Climate Data Center; http://www.wrcc.dri.edu/ summary/ climsmco.html) were used to define lapse rates in temperature and vertical precipitation gradients within the study area (Fig. 1, Table 2). Additional data for precipitation were obtained from seven SNOTEL stations. Where possible NCDC 1971–2000 norms are used. For shorter records (e.g., SNOTEL sites) or those with substantial discontinuities in the time series, period-of-record values are used but are weighted in proportion to the number of years for which reliable data exists between 1971 and 2000. Weighted least-squares regression reveals a significant linear variation of regional temperature data with elevation ($n = 14$, $r^2 = 0.67$, $p < 0.001$) which defines a lapse rate of ~0.0055 °C m^{-1} (Fig. 3b). (Without the weighting, or omitting altogether the non-NCDC norm values, the significance of the regression changes slightly but yields the same lapse rate.)

Regionally, changes in precipitation with elevation show a less obvious trend due in large part to a generally east–west precipitation gradient across the study area that presumably reflects an orographic effect ("rain shadow") on the prevailing westerly transport of moisture. Of note is that the crest of the Sawatch Range, which has the highest mean elevation of any range in Colorado, and the Taylor Park area are drier than their counterparts in the western Elk Mountains. Therefore, the precipitation data were segregated into groups corresponding to their approximate location (Table 2, Fig. 3c). The vertical precipitations gradients thus defined are ~0.0054 m w.e. m^{-1} for the Taylor Park area (including the eastern Elk Mountains; $n = 7$, $r^2 = 0.93$, $p < 0.001$), ~0.0088 m w.e. m^{-1} for the western Elk Mountains ($n = 7$, $r^2 = 0.88$, $p < 0.005$), and ~0.0027 m w.e. m^{-1} for the Arkansas Valley ($n = 7$, $r^2 = 0.72$, $p < 0.05$). Data from a SNOTEL site on Crested Butte mountain were not used; apart from appearing as an outlier on Figure 3c, its inclusion yielded a vertical precipitation gradient that resulted in modeled peak snowpack amounts (discussed subsequently) that substantially underestimate those observed. Again, unweighted regressions are virtually identical to those of the weighted regressions. The

TABLE 2

Modern temperature and precipitation data obtained from meteorological stations and SNOTEL sites within and adjacent to the study area. (See Fig. 1 for locations.)

Station	Elevation (m)	Mean annual temperature (°C)	Weighting for temperature values	Mean annual precipitation (m)	Weighting for precipitation values
Meteorological					
Arkansas Valley					
Salida	2182	7.3*	1.00	0.220*	1.00
Buena Vista	2422	6.2*	1.00	0.255*	1.00
Twin Lakes	2803	2.2*	1.00	0.251*	1.00
Sugarloaf	2968	1.3*	1.00	0.423*	1.00
Leadville	3029	1.6*	1.00	0.294*	1.00
Climax	3450	−0.7*	1.00	0.579*	1.00
Taylor Park area					
Gunnison	2329	2.9*	1.00	0.253*	1.00
Pitkin	2804	0.8	0.37	0.456	0.23
Taylor Park	2807	0.2*	1.00	0.431*	1.00
Independence Pass	3231	−0.3	0.17	0.700	0.13
Western Elk Mountains					
Meredith	2385	3.3*	1.00	0.415*	1.00
Redstone	2459	3.9	0.30	0.738	0.40
Aspen	2487	4.9*	1.00	0.591*	1.00
Crested Butte	2701	0.6*	1.00	0.606*	1.00
SNOTEL					
Taylor Park area					
Park Cone	2926			0.572	0.63
Independence Pass	3231			0.809	0.67
Brumley	3231			0.668	0.67
Western Elk Mountains					
North Lost Trail	2804			0.889	0.53
McClure Pass	2895			0.898	0.67
Schofield Pass	3261			1.245	0.53
Arkansas Valley					
Rough and Tumble	3158			0.480	0.50

* NCDC 1971–2000 normal.

reference elevation (z_{REF}) used for the Taylor Park area is 2800 m with the following values (obtained by regression of pertinent data): $T_a(z_{REF}) = 2.2$ °C; $T_{Jan}(z_{REF}) = -8.3$ °C; $T_{Jul}(z_{REF}) = 12.7$ °C; and $P(z_{REF}) = 0.49$ m w.e.; and for snow partitioning $c = 0.5$ and $T_{crit} = 1.5$ °C. That for the western Elk Mountains is 2600 m, using $T_a(z_{REF}) = 3.3$ °C; $T_{Jan}(z_{REF}) = -7.2$ °C; $T_{Jul}(z_{REF}) = 13.8$ °C; $P(z_{REF}) = 0.66$ m w.e.; and $c = 0.5$, and $T_{crit} = 3.0$ °C. For the Arkansas Valley, z_{REF} was chosen as 2400 m with $T_a(z_{REF}) = 4.4$ °C; $T_{Jan}(z_{REF}) = -6.4$ °C; $T_{Jul}(z_{REF}) = 15.2$ °C; $P(z_{REF}) = 0.24$ m w.e., and $c = 0.5$, and $T_{crit} = 2.0$ °C. The monthly distribution of precipitation follows the means of observations made at relevant stations.

Results and Discussion

ELAS OF RECONSTRUCTED GLACIERS

Eleven of the reconstructed glaciers used in the present paper have been presented previously (Brugger and Goldstein, 1999; Brugger, 2006) (see Fig. 2) and therefore the details are omitted here. The new reconstructions are shown in Figure 4 and their hypsometries (area-altitude distributions) and ELAs are shown graphically in Figure 5; all AAR-derived ELAs are tabulated in Table 3. The 22 ELAs derived from reconstructions in the study area together with 3 reported by Leonard (1989) for paleoglaciers on Snowmass Mountain (Elk Mountains), the eastern flank of the Sawatch Range, and western flank of the Mosquito Range define

a significant regional trend ($r^2 = 0.77$, $p < 0.001$) indicating an eastward rise of ~4.5 m km^{-1} (Fig. 6). This trend follows an inverse relationship to modern precipitation and therefore might suggest moisture sources, transport, and orographic effects on precipitation during the local LGM were similar to those today (Brugger and Goldstein, 1999). Within the Taylor Park area the mean ELA is 3370 ± 65 m ($n = 18$) whereas that in the western Elk Mountains is 3105 ± 100 m ($n = 4$).

MODEL VERIFICATION: MODERN SNOWPACK EVOLUTION AND ELAS

Following Brugger (2006), the validity of the DDM parameterization and its application to the study area is assessed in two ways: (1) its ability to accurately simulate the evolution of modern snowpack as recorded at SNOTEL sites; and (2) its prediction of modern regional ELA or snowline. Figures 7a–7g compare simulated evolution of snowpack to those recorded within the region of the study area. The model underestimates late spring snowpack by as much as 20% (Fig. 7f) and overestimates by as much as 35% (Fig. 7b). On average, however, the model underestimates snowpack by only ~5%. Disparities principally reflect: differences in the temporal resolution of the simulations (monthly) and observations (daily), resulting in differences in the timing of maximum snow accumulation (in some cases down-sampling of the SNOTEL records to a monthly resolution decreases these differences by a few percent); variations in the
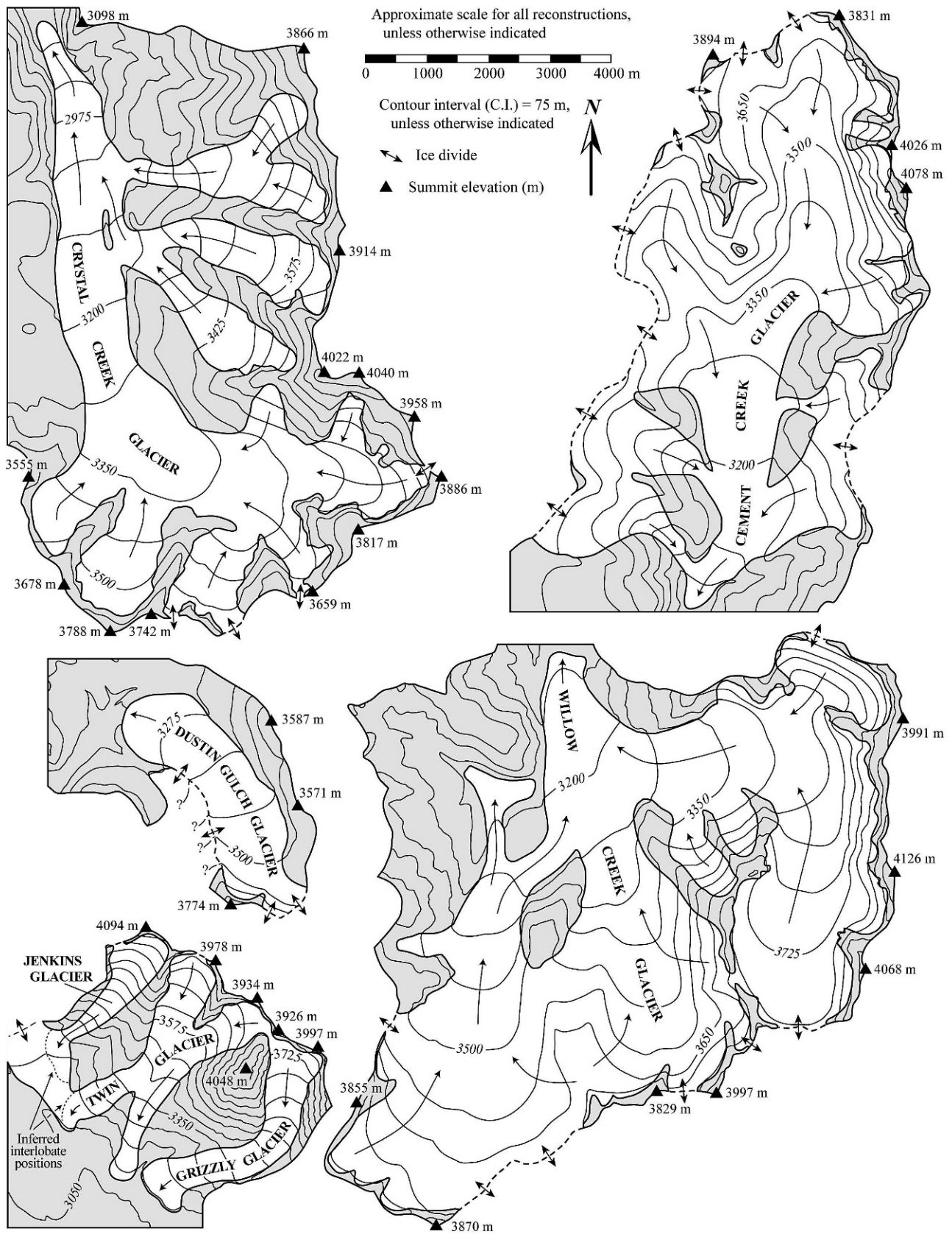
FIGURE 4. Reconstructed extent and ice-surface topography of the 11 paleoglaciers introduced in this study during the local last glacial maximum. Details of the other paleoglaciers used in this study were presented in Brugger and Goldstein (1999) and Brugger (2006).
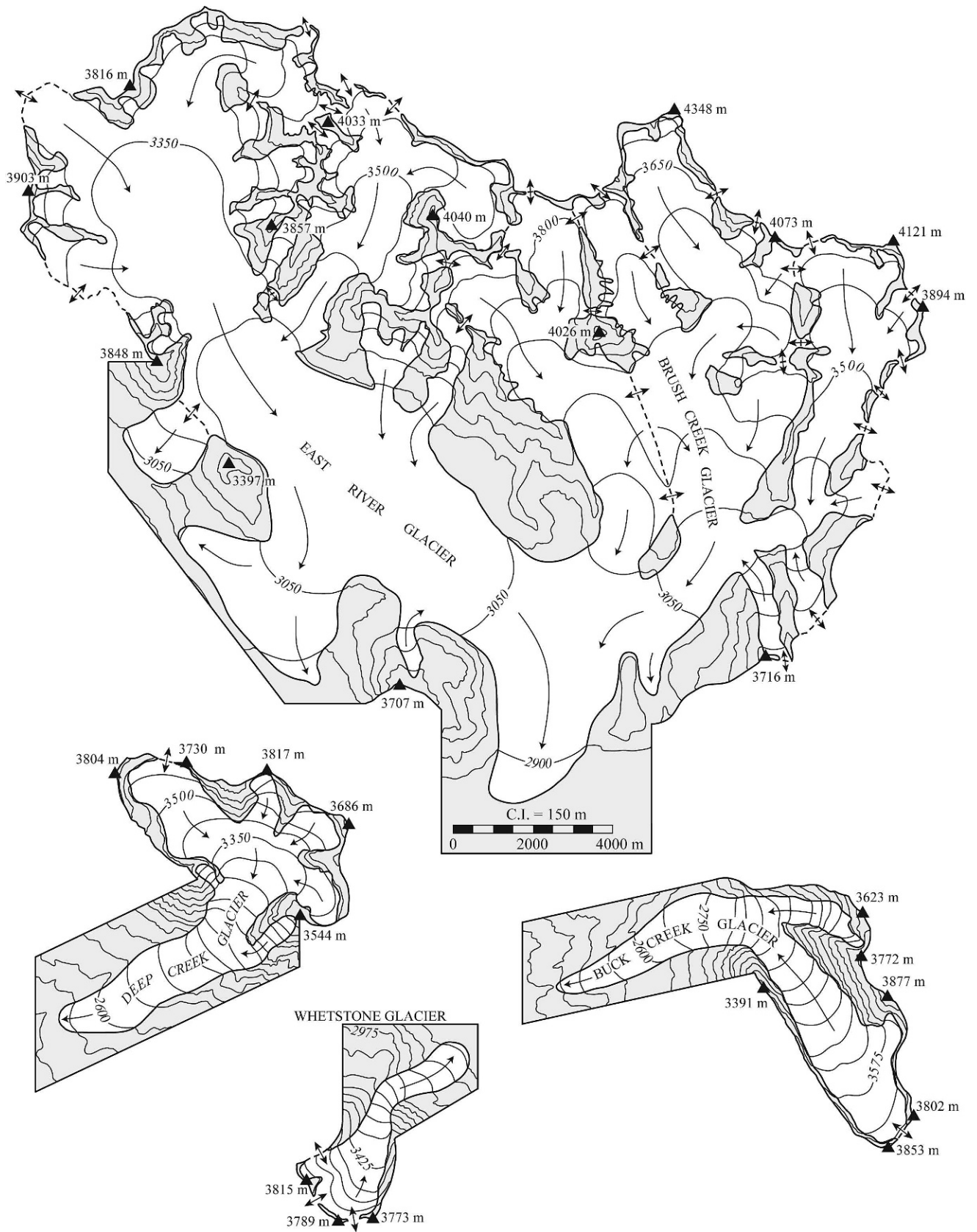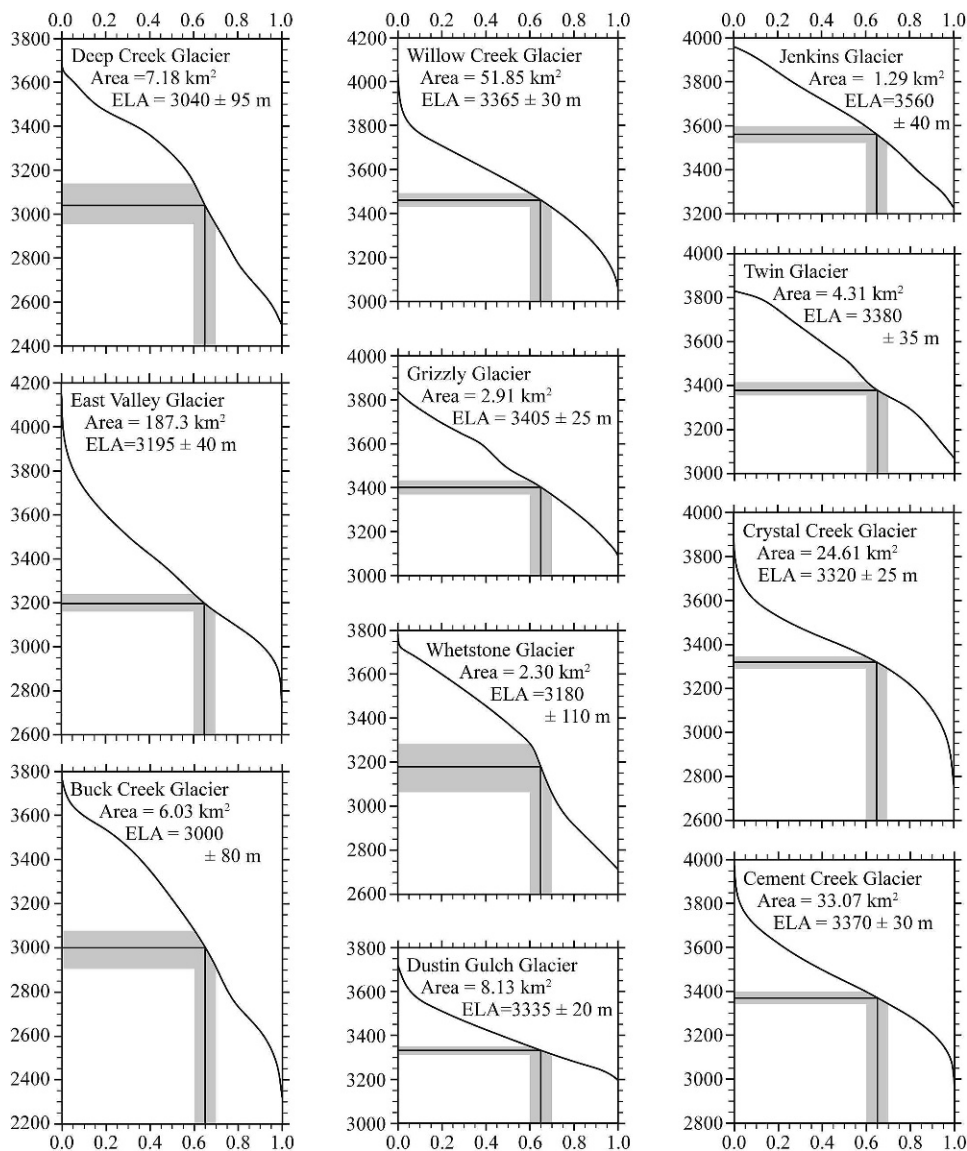
FIGURE 4. Continued.

FIGURE 5. Area-altitude distributions (hypsometries) of the 11 paleoglaciers introduced in this study and derived ELAs.

seasonal distribution of precipitation; and the regional nature of the regressions used to define the vertical precipitation gradients. In the Taylor Park area for example, the latter underestimates total precipitation at the Park Cone site by 6%. At the Independence Pass SNOTEL site, the model underestimates mean annual precipitation by 11%, but in fact overestimates that for the nearby meteorological station and the Brumley SNOTEL site by 2% and 7%, respectively. This underscores the spatial variability of precipitation, often problematic in mountainous terrain (Anderton et al., 2004), that is not accounted for in the model. It bears mentioning that a comparison of the period-of-record data for the SNOTEL sites with the corresponding observations at the meteorological stations indicates that the SNOTEL sites might overestimate mean annual precipitation, and therefore possibly snowpack, by up to ~10%. Finally, it is also worth noting that the variable forest canopy surrounding the SNOTEL sites adds an additional complexity for snow accumulation by either enhancing deposition or promoting wind deflation, and certainly might reduce insolation, decreasing d_f values to values lower than those considered here (Dingman, 2002). With regard to the latter, however, a d_f of 0.0025 m w.e. d^{-1} $°C^{-1}$, more representative of snow under tree canopy (Kuusisto, 1980) resulted in increases in

snowpack of only a few percent. In view of these considerations, the discrepancies between modeled and observed snowpack evolution are less serious than they might first appear.

The DDM yields modern ELAs, where $b_n = 0$, of 4405 ± 80 m in the Taylor Park area, 4170 ± 100 m in the western Elk Mountains, and 4645 ± 65 m in the Arkansas Valley. Modern ELAs are not known in the study area, but can be estimated using mean summer temperatures and mean annual precipitation. Ohmura et al. (1992) found that at the equilibrium lines of modern glaciers these two climatic parameters fall within a discrete envelope. Using a lapse rate of 0.0061 $°C$ m^{-1} based on mean summer temperatures (June, July, and August; $n = 14$, $r^2 = 0.85$, $p < 0.001$) and the vertical precipitation gradients previously given, modern climatic conditions that meet these criteria can be identified (Fig. 7h). These estimates are in excellent agreement with those derived from the DDM. It is also consistent with observations of the location and persistence of snowfields on the higher peaks (~4200–4450 m) in and surrounding the study area. Although these snowfields are not strictly perennial—for example, they virtually disappeared during the summer of 2002—only a few persist for any number of summers and only then in favorable topographic settings. Thus, these snowfields reflect local (or

TABLE 3

Equilibrium-line altitudes (ELAs), accumulation-area ratios (AARs), and temperature depression derived using the degree-day model and a steady-state glacier mass balance approach.

Glacier	AAR-derived ELA* (m)	ELA* (m) required for steady-state ($B_n = 0$)	Implied temperature depression** (°C)	Equivalent AAR	$ELA_{AAR} - ELA_{SSMB}$[†] (m)
Taylor Park/Eastern Elk Mts.					
Cement Creek	3370 ± 30	3395	6.7	0.61	−25
Crystal Creek	3320 ± 25	3310	7.2	0.66	10
Willow Creek	3365 ± 30	3470	6.2	0.64	−5
Dustin Gulch	3335 ± 20	3365	7.0	0.56	−30
Grizzly	3405 ± 25	3420	6.5	0.63	−15
Twin	3380 ± 35	3430	6.4	0.60	−60
Jenkins	3560 ± 40	3580	5.4	0.62	−20
Taylor River Lobe	3400 ± 50	3410	6.6	0.64	−10
Spring Creek Lobe	3280 ± 40	3335	7.1	0.59	−55
Rocky Brook	3395 ± 10	3415	6.6	0.55	−20
Trail Creek	3340 ± 45	3355	7.0	0.64	−15
Bushwhack	3275 ± 35	3305	7.3	0.60	−30
Texas Creek	3385 ± 50	3300	7.3	0.63	85
Pass Creek	3375 ± 40	3395	6.7	0.61	−20
Cow Creek	3350 ± 40	3380	6.8	0.61	−30
Sanford Creek	3435 ± 40	3420	6.5	0.67	15
Lottis Creek	3340 ± 30	3350	7.0	0.64	−10
South Lottis Creek	3375 ± 30	3320	7.2	0.69	55
Means	3370 ± 60	3385 ± 70	6.8 ± 0.5	0.62 ± 0.05	−10 ± 35
Western Elk Mts.					
East Valley	3195 ± 95	3270	6.3	0.57	−75
Whetstone	3180 ± 110	3185	6.9	0.65	−5
Buck Creek	3000 ± 80	3015	8.2	0.64	−15
Deep Creek	3040 ± 95	3050	7.9	0.64	−10
Means	3105 ± 100	3130 ± 120	7.3 ± 0.9	0.63 ± 0.04	−25 ± 35
Mean temperature depression for the broader Taylor Park/Elk Mts. region			6.9 ± 0.6		

* Reported to the nearest 5 m.

** Reported to the nearest 0.1 °C.

[†] AAR-derived ELA minus ELA determined by steady-state mass balance. Reported to the nearest 5 m.

orographic) snowline(s) and suggest regional snowline lies at an elevation close to, but above the highest summits.

LATE GLACIAL CLIMATE INFERRED FROM DEGREE-DAY MODELING

The first approach used to infer LGM climate change in the study area was to find values of ΔT_{Jul}, ΔT_{Jan}, and F_p that would yield ELAs equal to the mean ELAs independently derived from the reconstructed glaciers in each of the Taylor Park and western Elks regions, 3370 ± 65 m and 3100 ± 105 m, respectively. Initial runs were such that a uniform temperature depression (ΔT, = $\Delta T_{Jul} = \Delta T_{Jan}$) was applied and assuming LGM precipitation was comparable to that today (i.e., $F_p = 1.0$). Under these prescribed conditions a temperature depression of ~6.8 °C is required to lower ELA in the Taylor Park region to its presumed LGM value of 3370 m (Fig. 8a). Similarly, a cooling of ~7.5 °C is required to lower ELA to 3105 m in the western Elk Mountains. For both areas uncertainties in ELA estimates and d_f each contribute to an uncertainty in ΔT on the order ±0.5 °C, and from Figure 8a the combined uncertainty probably does not exceed about 1.0 °C. Thus, the modeling results suggest comparable LGM cooling in the broader region.

Another set of modeling runs allowed F_p to vary between 0.5 and 2.0, thus examining LGM scenarios in which precipitation differed from modern climate. The motivation for these simula-

tions is twofold. First, a common feature of general circulation models (GCMs) of LGM climate (e.g., Kutzbach et al., 1993; Bartlein and Hostetler, 2004) is that a bifurcation of the jet stream led to wetter climates in the (now) desert southwestern U.S.A. At the same time easterly flow, driven by a glacial cyclone over the Laurentide Ice Sheet, created drier conditions over the Pacific Northwest and northern Rocky Mountains. This general pattern of circulation is furthermore supported by synoptic summaries of paleoclimate proxies (Thompson et al., 1993; Bartlein et al., 1998). Regional climate modeling by Hostetler and Clark (1997) also suggests that LGM climate in the Central Rocky Mountains might have been somewhat drier. Modeling by Bartlein et al. (1998) and Hostetler and Bartlein (1999), however, indicates the possibility of increased July precipitation (or at least wetter surface environments) in the Central Rockies, but the southern Sawatch Range lies along the boundary between slightly wetter and slightly drier conditions during January. Wetter LGM conditions might also be reflected in a pollen record from the nearby Front Range (Legg and Baker, 1980). Thus, given the limitations of the spatial resolution of the modeling and the paucity of proxies for paleoprecipitation, there remain the possibilities that LGM climate was slightly drier or wetter in the study area.

In addition to examining temperature depression in conjunction with possible wetter/drier LGM climates, a second reason for varying precipitation was to test the sensitivity of the simulations to potential inaccurate and/or incomplete parameterizations that
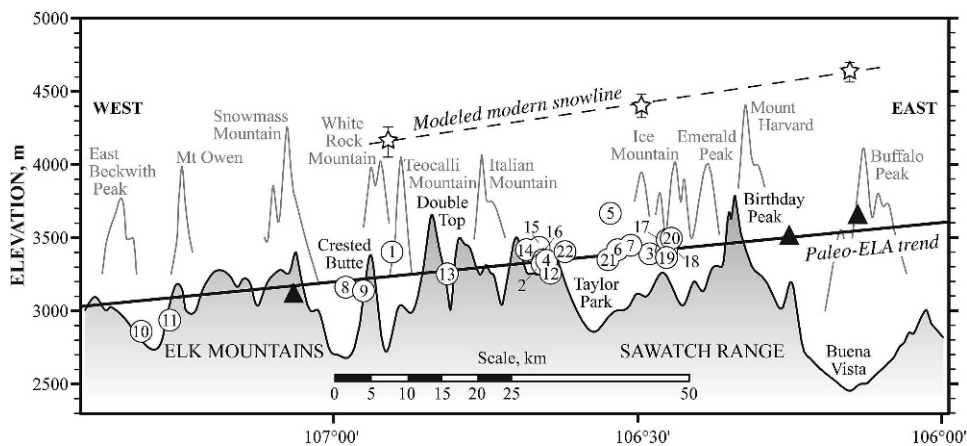
FIGURE 6. LGM and model-simulated modern ELA trends along an east–west cross section through study area. Numbers in circled points correspond to the paleoglaciers identified in Figure 2, triangles are LGM ELAs reported by Leonard (1989), and stars are estimates of modern ELAs with model uncertainties shown. Topography is generalized, and individual peaks are shown to convey the terrain in the study area.

may lead to erroneous amounts of accumulation. These could include those in: (1) estimates of modern mean annual precipitation, particularly at the reference elevation; (2) the precise formulation of the partition function f that determines the fraction of monthly precipitation that falls as snow; (3) changes in the seasonal distribution of (as opposed to total) precipitation during the LGM; and (4) any additional (internal) accumulation resulting from the refreezing of meltwater that are not accounted for in the model. For example, changing annual precipitation in the simulations is equivalent to changing the snow/rain fractionation of monthly precipitation [Equation (6)] that in turn would increase or decrease accumulation. Alternatively, such changes represent LGM scenarios wherein changes in seasonal distribution of precipitation could have led to either wetter or drier winters than those presupposed in simulations.

It is quite likely that any changes in LGM precipitation totals or its seasonal distribution were modest, and similarly errors introduced by the parameterizations are probably small. Therefore, simulations using F_p of 1.25 and 0.75 are thought to yield a liberal estimate of the uncertainty in the derived temperature depression associated with these factors. Figure 7b shows that in the Taylor Park region this uncertainty is $\sim \pm 0.3$ °C. Even if LGM climate was substantially wetter ($F_p = 1.5$) or drier ($F_p = 0.5$) winters—a situation not supported by any existing regional paleoclimate proxy—or other factors greatly affected accumulation, this uncertainty only increases to approximately ± 0.9 °C. The same conclusions are suggested by comparable simulations for the western Elk Mountains.

An additional sensitivity analysis was performed to explore the effect of increased temperature seasonality ($\Delta T_{Jul} \neq \Delta T_{Jan}$) during the LGM. Such increases are indicated by fossil beetle assemblages (Elias, 1996) that suggest mean January temperatures could have been as much as 30 °C colder than present. In contrast, regional climate modeling (Hostetler and Bartlein, 1999) suggests LGM January air temperatures were comparable to those today. Two modeling scenarios (again for the Taylor Park region, Fig. 7c) were used to bracket these possibilities, specifically allowing ΔT_{Jan} to have fixed values of -30 and 0 °C. These nonuniform changes in ΔT_{Jan} and ΔT_{Jul} effectively change the length of the ablation season (shortening and lengthening, respectively) and alter total accumulation (increase and decrease, respectively) by virtue of changing the mean monthly temperature in early fall and late spring months when it is more critical in determining the fraction of precipitation that falls as snow. The resulting uncertainties introduced by potential changes in temperature seasonality are about ± 1.0 °C. Sensitivity analyses also

reveal that uncertainties associated with the temperature lapse rate and vertical precipitation gradient (taken as ± 0.0005 °C m^{-1} and ± 0.005 cm w.e. m^{-1}, respectively) are also small, being ± 0.3 °C for the former and ± 0.1 °C for the latter.

The second approach used to infer LGM climate change in the study area involved finding values of ΔT required to maintain steady-state mass balance ($B_n = 0$) for the 22 paleoglaciers. Because of the robustness of the ΔT values derived from the DDM, despite the different scenarios and uncertainties discussed above, no effort was made to systematically examine the effect of varying F_p, seasonality, and so forth in these simulations. Table 3 summarizes the results. The required temperature depressions range from a minimum value of 5.4 °C (Jenkins glacier) to a maximum of 8.2 °C (Buck Creek glacier). The respective means from the Taylor Park/eastern Elk Mountains and western Elk Mountains of 6.8 $\pm$ 0.5 and 7.3 $\pm$ 0.9 °C are both regionally consistent and are in excellent agreement with that found using the mean of the AAR–derived ELAs (6.8 and 7.5 °C). Assuming that across the broader region LGM temperature depression was the same, these results suggest that this was 6.9 $\pm$ 0.6 °C.

Also shown in Table 3 are the ELAs and AARs associated with the condition of steady-state mass balance for the reconstructed paleoglaciers. The mean ELAs in each region (3385 $\pm$ 70 and 3130 $\pm$ 120 m) are remarkably consistent with those derived from the AAR method. In general, the range of AARs associated with the simulation of steady-state mass balances of the glaciers falls within or very close to that assumed in applying the AAR method of ELA determination, namely 0.65 $\pm$ 0.05.

These estimates of LGM temperature change determined by degree-day modeling are comparable with others determined in the Central and Southern Rocky Mountain region. In the study area, Brugger and Goldstein (1999) suggested a cooling of between 7 and 9 °C using an analysis of ELA depression in the context of climate at the equilibrium line of modern glaciers. In the nearby Sangre de Cristo Range, LGM ELAs suggest mean summer temperatures were depressed ~ 7–8 °C (Refsnider et al., 2009). Similar analyses allowed Leonard (1989) to conclude that barring any changes in precipitation, LGM temperatures were ~ 8.5 °C cooler in the Colorado Rocky Mountains. In the Uinta Mountains in Utah, Munroe and Mickelson (2002) and Refsnider et al. (2008) showed that a cooling in the range of 5–7 °C was sufficient to support LGM glaciers under presumed local enhancement of precipitation due to the presence of Glacial Lake Bonneville. In the Uinta and Wasatch Mountains, Laabs et al. (2006) inferred a 6–7 °C temperature depression during the LGM based on a coupled energy balance–glacial flow model, again assuming
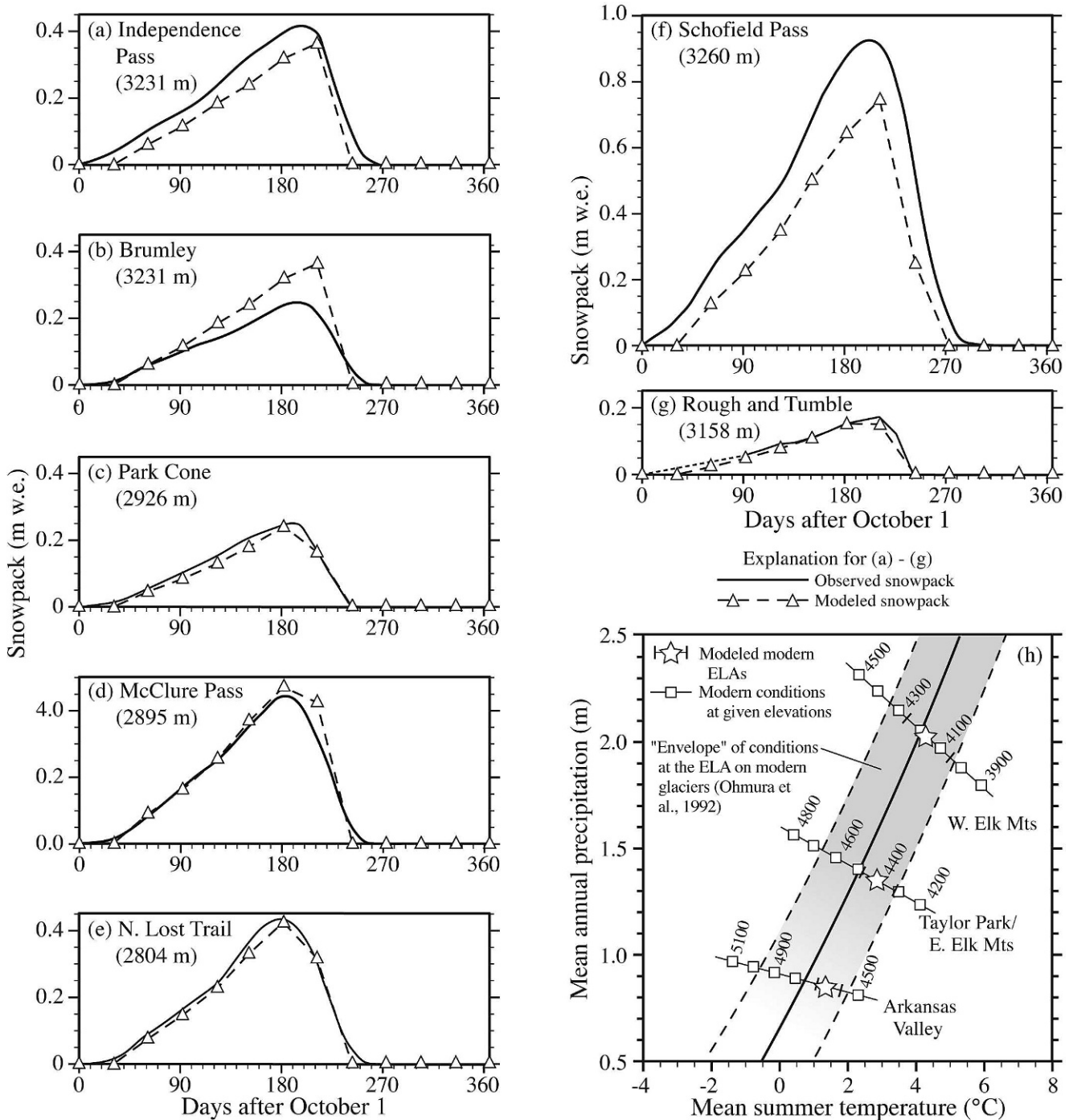
FIGURE 7. (a)–(g) Simulated and observed evolution of modern snowpack at SNOTEL sites. Solid lines are observed daily variations, dashed lines are modeled monthly variations. See text for discussion. (h) Estimates of modern ELA based on temperature and precipitation at glacier equilibrium lines and simulated by degree-day modeling. After Ohmura et al. (2001) and Brugger (2006).

enhanced local precipitation. The spatial resolution notwithstanding, climate modeling by Hostetler and Clark (1997) suggests LGM temperatures 9–12 °C lower than today in the Southern and Central Rocky Mountains, and subsequent modeling by Hostetler and Bartlein (1999) suggests temperature depression of between 4 and 8 °C in the region of study area. More recently, Leonard (2007) found that mean summer temperatures between ~6 and 8 °C cooler than present would have been sufficient to maintain the LGM extents of glaciers in the major ranges of Wyoming and Colorado, and in Utah if local precipitation was enhanced.

Degree-day modeling also underscores the importance of the depression of summer temperature in driving glaciation within the region; that is lowering of equilibrium lines appears to be less sensitive to changes in precipitation and winter temperature. This dependence on summer temperatures was noted previously by Leonard (1989, 2007), Hostetler and Clark (1997), Brugger and Goldstein (1999), and Brugger (2006). For the study area in particular, the present work and that of Brugger (2006) shows that if mean summer temperature were, say, 5 to 6 °C as opposed to ~7 °C cooler, the precipitation required would have had to have been
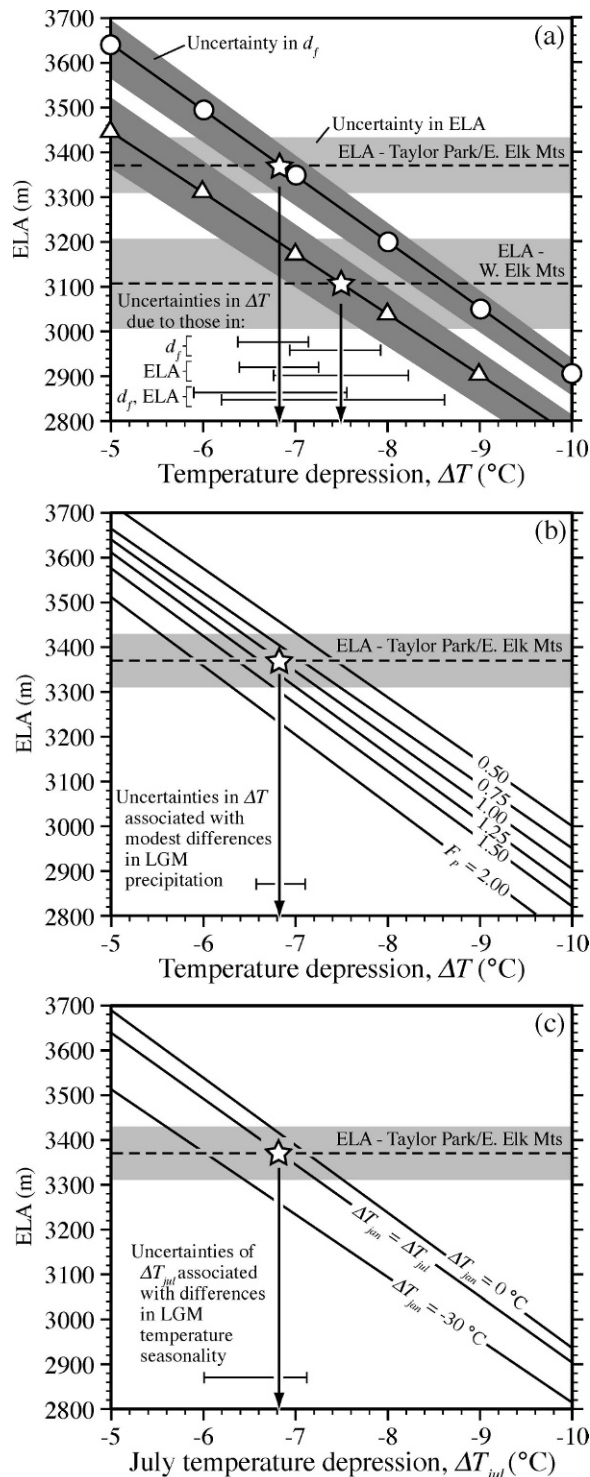
FIGURE 8. (a) Variation of ELA with prescribed uniform temperature depression ΔT ($\Delta T_{jul} = \Delta T_{jan}$) assuming LGM precipitation was comparable to that today ($F_p = 1.0$). Horizontal dashed line is mean paleo-ELA obtained from the glacier reconstructions, and shaded area is the associated standard deviation in the areas of Taylor Park and the western Elk Mountains. (b) Variation of ELA with ΔT and possible changes in LGM precipitation in the Taylor Park region. F_p values are expressed as fractional changes with respect to modern precipitation. (c) Variation of ELA with ΔT_{jul} assuming differences in LGM temperature seasonality ($\Delta T_{jul} \neq \Delta T_{jan}$) and precipitation was comparable to that today ($F_p = 1.0$).

2–3 times more than that today. Such changes are not indicated by any paleoclimate proxies or modeling.

Conclusions

LGM ELAs for 22 reconstructed glaciers in the southern Sawatch Range and Elk Mountains ranged from 3000 to 3560 m, rising eastward along a statistically significant trend of ~4.5 m km^{-1}. Within the Taylor Park region the mean ELA is 3370 ± 60 m, and that within the western Elk Mountains is 3130 ± 120 m. Degree-day modeling suggests that without any appreciable change in precipitation, the LGM extent of paleoglaciers in the study area would have supported by depression of mean summer temperatures between ~5.4 and 8.2 °C. Regionally, the temperature depression during the LGM is inferred to have been about 7 °C. Modeling also implies that these estimates of temperature change are not overly dependent on potential changes in either LGM precipitation or temperature seasonality. Nor are they especially sensitive to uncertainties in model parameterization. These results are consistent with previous estimates of LGM climate change within the Southern and Central Rocky Mountain region in terms of both the magnitude and importance of summer temperature depression in driving and maintaining glaciation.

Acknowledgments

References Cited

Anderton, S. P., White, S. M., and Alvera, B., 2004: Evaluation of spatial variability in snow water equivalent for a high mountain catchment. *Hydrologic Processes*, 18: 435–453.

Bartlein, P. J., and Hostetler, S. W., 2004: Modeling paleoclimates. *In* Gillespie, A. R., Porter, S. C., and Atwater, B. F. (eds.), *The Quaternary Period in the United States*. Amsterdam: Elsevier, 565–584.

Bartlein, P. J., Anderson, K. H., Anderson, P. M., Edwards, M. E., Mock, C. J., Thompson, R. S., Webb, R. S., Webb, T., III, and Whitlock, C., 1998: Paleoclimatic simulations for North America over the past 21,000 years: features of the simulated climate and comparisons with paleoenvironmental data. *Quaternary Science Reviews*, 17: 549–585.

Braithwaite, R. J., 1995: Positive degree-day factors for ablation on the Greenland ice sheet studied by energy-balance modelling. *Journal of Glaciology*, 41: 153–160.

Braithwaite, R. J., and Olesen, O. B., 1989: Calculation of glacier ablation from air temperature, West Greenland. *In* Oerlemans, J. (ed.), *Glacier Fluctuations and Climate Change*. Dordrecht: Kluwer Academic Publishers, 219–233.

Braithwaite, R. J., and Olesen, O. B., 1993: Seasonal variation of ice ablation at the margin of the Greenland ice sheet and its sensitivity to climate change, Qamanârssûp sermia, West Greenland. *Journal of Glaciology*, 39: 267–274.

Braithwaite, R. J., and Raper, S. C. B., 2002: Glaciers and their contribution to sea level change. *Physics and Chemistry of the Earth*, 27: 1445–1454.

Braithwaite, R. J., and Zhang, Y., 1999: Modelling changes in glacier mass balance that may occur as a result of climate changes. *Geografiska Annaler*, 81A: 489–496.

Braithwaite, R. J., and Zhang, Y., 2000: Sensitivity of mass balance of five Swiss glaciers to temperature changes assessed by tuning a degree-day model. *Journal of Glaciology*, 46: 7–14.

Brugger, K. A., 2006: Late Pleistocene climate inferred from the reconstruction of the Taylor River Glacier Complex, southern Sawatch Range, Colorado. *Geomorphology*, 75: 318–329.

Brugger, K. A., 2007: Cosmogenic ^{10}Be and ^{36}Cl ages from late Pleistocene terminal moraine complexes in the Taylor River drainage basin, central Colorado, U.S.A. *Quaternary Science Reviews*, 26: 494–499.

Brugger, K. A., and Goldstein, B. S., 1999: Paleoglacier reconstruction and late-Pleistocene equilibrium-line altitudes, southern Sawatch Range, Colorado. *In* Mickelson, D. M., and Attig, J. W. (eds.), *Glacial Processes Past and Present.* Geological Society of America Special Paper, 337: 103–112.

Casal, T. G. D., Kutzback, J. E., and Thompson, L. G., 2004: Present and past ice-sheet mass balance simulations for Greenland and the Tibetan Plateau. *Climate Dynamics*, 23: 407–425.

deWoul, M., and Hock, R., 2005: Static mass-balance sensitivity of Arctic glaciers and ice caps using a degree-day approach. *Annals of Glaciology*, 42: 217–224.

Dingman, S. L., 2002: *Physical Hydrology.* Second edition. Upper Saddle Brook: Prentice Hall.

Elias, S. A., 1996: Late Pleistocene and Holocene seasonal temperatures reconstructed from fossil beetle assemblages in the Rocky Mountains. *Quaternary Research*, 46: 311–318.

Flowers, G. E., Marshall, S. J., Björnsson, H., and Clarke, G. K. C., 2005: Sensitivity of Vatnajökull ice cap hydrology and dynamics to climate warming over the next 2 centuries. *Journal of Geophysical Research*, 110: article F02011.

Hock, R., 1999: A distributed temperature-index ice- and snowmelt model including potential direct solar radiation. *Journal of Glaciology*, 45: 101–111.

Hock, R., 2003: Temperature index melt modelling in mountain areas. *Journal of Hydrology*, 282: 104–115.

Hostetler, S. W., and Bartlein, P. J., 1999: Simulation of the potential responses of regional climate and surface processes in western North America to a canonical Heinrich event. *In* Clark, P. U., Webb, R. S., and Keigwin, L. D. (eds.), *Mechanism of Global Climate Change at Millennial Timescales.* American Geophysical Union Geophysical Monograph, 12: 313–327.

Hostetler, S. W., and Clark, P. U., 1997: Climatic controls of western U.S. glaciers at the last glacial maximum. *Quaternary Science Reviews*, 16: 505–511.

Hostetler, S. W., and Clark, P. U., 2000: Tropical climate at the last glacial maximum inferred from glacier mass-balance modeling. *Science*, 290: 1747–1750.

Hughes, P. D., and Braithwaite, R. J., 2008: Application of a degree-day model to reconstruct Pleistocene glacial climates. *Quaternary Research*, 69: 110–116.

Huybrechts, P., 2002: Sea-level changes at the LGM from ice-dynamic reconstructions of the Greenland and Antarctic ice sheets during the glacial cycles. *Quaternary Science Reviews*, 21: 203–231.

Huybrechts, P., and Oerlemans, J., 1990: Response of the Antarctic ice sheet to future greenhouse warming. *Climate Dynamics*, 5: 93–102.

Jóhannesson, T., 1997: The response of two Icelandic glaciers to climatic warming computed with a degree-day glacier mass balance model couple to a dynamic glacier model. *Journal of Glaciology*, 43: 321–337.

Jóhannesson, T. O., Siggurdsson, O., Laumann, T., and Kennett, M., 1995: Degree-day glacier mass balance modelling with applications to glaciers in Iceland, Norway, and Greenland. *Journal of Glaciology*, 41: 345–358.

Kayastha, R. B., Ageta, Y., Nakawo, M., Fujita, K., Sakai, A., and Matsuda, Y., 2003: Positive degree-day factors for ice ablation on four glaciers in the Nepalese Himalayas and Qinghai-Tibetan Plateau. *Bulletin of Glaciological Research*, 20: 7–14.

Klein, A. P., Seltzer, G. O., and Isacks, B., 1999: Modern and last local glacial maximum snowlines in the Central Andes of Peru, Bolivia, and northern Chile. *Quaternary Science Reviews*, 18: 63–84.

Kull, C., and Grosjean, M., 2000: Late Pleistocene climate conditions in the north Chilean Andes drawn from a climate-glacier model. *Journal of Glaciology*, 46: 622–632.

Kutzbach, J. E., Guetter, P. J., Behling, P. J., and Selin, R., 1993: Simulated climate changes: results of the COHMAP climate-model experiments. *In* Wright, H. E., Kutzbach, J. E., and Webb, T., III (eds.), *Global Climates since the Last Glacial Maximum.* Minneapolis: University of Minnesota Press, 24–93.

Kuusisto, E., 1980: On the values and variability of degree-day melting factor in Finland. *Nordic Hydrology*, 11: 235–242.

Laabs, B. J. C., Plummer, M. A., and Michelson, D. M., 2006: Climate during the last glacial maximum in the Wasatch and southern Uinta Mountains inferred from glacial modeling. *Geomorphology*, 75: 300–318.

Laumann, T., and Reeh, N., 1993: Sensitivity to climate change of the mass balance of glaciers in southern Norway. *Journal of Glaciology*, 39: 656–665.

Legg, T. E., and Baker, R. G., 1980: Palynology of Pinedale sediments, Devlin Park, Boulder County, Colorado. *Arctic and Alpine Research*, 12: 319–333.

Leonard, E., 2007: Modeled patterns of late Pleistocene glacier inception and growth in the Southern and Central Rocky Mountains, USA: sensitivity to climate change and paleoclimatic implications. *Quaternary Science Reviews*, 26: 2156–2166.

Leonard, E. M., 1989: Climate change in the Colorado Rocky Mountains: estimates based on modern climates at late Pleistocene equilibrium lines. *Arctic and Alpine Research*, 21: 245–255.

Licciardi, J. M., Clark, P. U., Brook, E. J., Elmore, D., and Sharma, P., 2004: Variable responses of western U.S. glaciers during the last deglaciation. *Geology*, 32: 81–84.

Marshall, S. J., James, T. S., and Clarke, G. K. C., 2002: North American ice sheet reconstructions at the Last Glacial Maximum. *Quaternary Science Reviews*, 21: 175–192.

Meierding, T. C., 1982: Late Pleistocene glacial equilibrium-line altitudes in the Colorado Front Range: a comparison of methods. *Quaternary Research*, 18: 289–310.

Miller, M. M., and Pelto, M. S., 1999: Mass balance measurements on the Lemon Creek Glacier, Juneau Icefield, Alaska 1953–1998. *Geografiska Annaler*, 81A: 671–681.

Munroe, J. S., and Mickelson, D. M., 2002: Last glacial maximum equilibrium-line altitudes and paleoclimate, northern Uinta Mountains, Utah, USA. *Journal of Glaciology*, 48: 257–266.

Munroe, J. S., Laabs, B. J. C., Shakun, J. D., Singer, B. S., Mickelson, D. M., Refsnider, K. A., and Caffee, M. W., 2006: Latest Pleistocene advance of alpine glaciers in the southwestern Uinta Mountains, northeastern Utah, USA: evidence for the influence of local moisture sources. *Geology*, 34: 841–844.

Naruse, R., Skvarca, P., and Takeuchi, Y., 1997: Thinning and retreat of Glaciar Upsala, and an estimate of annual ablation changes in southern Patagonia. *Annals of Glaciology*, 24: 38–42.

Oerlemans, J., Anderson, B., Hubbard, A., Huybrechts, P., Jóhannesson, T., Knap, W. H., Schmeits, M., Stroeven, A. P., van de Wal, R. S. W., Wallinga, J., and Zuo, Z., 1998: Modelling the response of glaciers to climate warming. *Climate Dynamics*, 14: 267–274.

Ohmura, A., 2001: Physical basis for the temperature-based melt-index method. *Journal of Applied Meteorology*, 40: 753–761.

Ohmura, A., Kasser, P., and Funk, M., 1992: Climate at the equilibrium line of glaciers. *Journal of Glaciology*, 38: 397–411.

Ohno, H., and Nakawo, M., 1998: Heat budget of a snow pack. *In* Nakawo, M., and Hayakawa, N. (eds.), *Snow and Ice Science in Hydrology*. Nagoya: Nagoya University, 69–88.

Oldfield, F., and Alverson, K., 2003: The societal relevance of paleoenvironmental research. *In* Alverson, K. D., Bradley, R. S., and Pederson, T. F. (eds.), *Paleoclimate, Global Change and the Future*. Berlin: Springer-Verlag, 1–10.

Östling, M., and Hooke, R. LeB., 1986: Water storage in Storglaciären, Kebnekaise, Sweden. *Geografiska Annaler*, 68A: 279–290.

Outcalt, S. I., and MacPhail, D. D., 1965: *A Survey of Neoglaciation in the Front Range of Colorado*. Boulder: University of Colorado Press.

Paterson, W. S. B., 1994: *The Physics of Glaciers*. Oxford: Pergamon Press.

Pierce, K. L., 2004: Pleistocene glaciation of the Rocky Mountains. *In* Gillespie, A. R., Porter, S. C., and Atwater, B. F. (eds.), *The Quaternary Period in the United States*. Amsterdam: Elsevier, 63–76.

Porter, S. C., 1975: Equilibrium line altitudes of late Quaternary glaciers in the Southern Alps, New Zealand. *Quaternary Research*, 5: 27–47.

Pytte, R., and Liestøl, O., 1966: Glasio-hydrologiske undersøkelser i Norge 1965. NVE årsrapport fra Brekontoret.

Raper, S. C. B., and Braithwaite, R. J., 2006: Low sea level rise projections from mountain glaciers and icecaps under global warming. *Nature*, 439: 311–313 (doi:10.1038/nature04448).

Raper, S. C. B., Brown, O., and Braithwaite, R. J., 2000: A geometric glacier model for sea-level change calculations. *Journal of Glaciology*, 46: 357–368.

Refsnider, K., and Brugger, K. A., 2001: Determination of degree-day factors and mass balance simulation on Rabots Glaciär, Swedish Lapland. *Geological Society of America Abstracts with Programs*, 33: A13.

Refsnider, K., Brugger, K. A., Leonard, E. M., McCalpin, J. P., and Armstrong, P. P., 2009: Last glacial maximum equilibrium-line altitude trends and precipitation patterns in the Sangre de Cristo Mountains, southern Colorado, USA. *Boreas*, 38: 663–678.

Refsnider, K. A., Laabs, B. J. C., Plummer, M. A., Singer, B. S., Mickelson, D. M., and Caffee, M. W., 2008: Last glacial maximum climate inferences from cosmogenic dating and glacier modeling of the western Uinta ice field, Uinta Mountains, Utah. *Quaternary Research*, 59: 130–144.

Tangborn, W. V., 1999: A mass balance model that uses low-altitude meteorological observations and the area-altitude distribution of a glacier. *Geografiska Annaler*, 81A: 753–766.

Thackray, G. D., Lundeen, K. A., and Borgert, J. A., 2004: Latest Pleistocene alpine glacier advances in the Sawtooth Mountains, Idaho, U.S.A.: reflection of mid-latitude moisture transport at the close of the last glaciation. *Geology*, 32: 225–228.

Thompson, R. S., Whitlock, C., Bartlein, P. J., Harrison, S. P., and Spalding, W. G., 1993: Climatic changes in the western United States since 18,000 yr B.P. *In* Wright, H. E., Kutzbach, J. E., and Webb, T., III (eds.), *Global Climates since the Last Glacial Maximum*. Minneapolis: University of Minnesota Press, 468–513.

Torsnes, I., Rye, N., and Nesje, A., 1993: Modern and Little Ice Age equilibrium-line altitudes on outlet valley glaciers from Jostedalsbreen, western Norway: an evaluation of different approaches to their calculation. *Arctic and Alpine Research*, 25: 106–116.

Trabant, D. C., and Mayo, L. R., 1985: Estimation of internal accumulation on five glaciers in Alaska. *Annals of Glaciology*, 6: 113–117.

Vincent, C., 2002: Influence of climate change over the 20th century on four French glacier mass balances. *Journal of Geophysical Research*, 107: ACL4.1–ACL4.12.

Vincent, C., Le Meur, E., and Delphine, S., 2005: Solving the paradox of the end of the Little Ice Age in the Alps. *Journal of Geophysical Research*, 32: L09706–L09709.

Whetton, P. H., Haylock, M. R., and Galloway, R., 1996: Climate change and snow-cover duration in the Australian Alps. *Climate Change*, 32: 447–479.

Wild, M., Pieluigi, C., Scherrer, S. C., and Ohmura, A., 2003: Effects of polar ice sheets on global sea level in high resolution greenhouse scenarios. *Journal of Geophysical Research*, 108: No D5, 4165, doi: 10.1029/2002JD002451.

Woo, M., and Fitzharris, B. B., 1992: Reconstruction of mass balance variations for Franz Josef Glacier, New Zealand, 1913–1989. *Arctic and Alpine Research*, 24: 281–290.